

# Phonon condensation and cooling via nonlinear feedback

Xu Zheng<sup>1,\*</sup> and Baowen Li<sup>2,1,†</sup>

<sup>1</sup>*Department of Physics, University of Colorado, Boulder, CO, 80309, USA*

<sup>2</sup>*Paul M. Rady Department of Mechanical Engineering,  
University of Colorado, Boulder, CO, 80309, USA*

(Dated: January 4, 2022)

We show that in multimode mechanical systems, the amplification of the lowest mode and the damping of all the other modes can be realized simultaneously via nonlinear feedback. The feedback-induced dynamics of the multimode system is related to the formation of phonon condensation. The phonon statistics of the lowest mode are similar to those of a phonon laser. Finally, we show the coherence of the lowest mode can be improved by an order of magnitude.

*Introduction.* – Manipulation and control of both coherent and incoherent phonons and/or vibration energy is of great interest for both engineering applications and fundamental research. On the one hand, the coherent phonons and/or vibrations shows great potential in applications ranging from conventional nondestructive testing [1, 2], high resolution imaging and sensing [3], to quantum information transfer and storage, etc [4–6]. On the other hand, the control of incoherent phonons and/or vibrations is of primary importance in noise reduction [7], thermoelectric energy conversion [8], heat management such as heat dissipation and heat insulation [9, 10].

In applications like highly sensitive and ultra-fast sensing [11–13], acoustic actuation [14–16], information processing [17–19], biological imaging [20–22], amplifying vibration amplitude and narrowing phonon linewidth are critical for good performance. Active linear feedback control, namely, feedback force is proportional to the measured mechanical displacement or velocity but with a phase difference, is a well-known technique for achieving these two goals. The control consists of the real-time monitoring of mechanical motion and feedback loop. Depending on the phase difference, either positive or negative feedback can be realized. This technique works well when the resonator can be considered as a single mode system.

In general, however, mechanical resonators have a series of normal modes. A single linear feedback loop results in the simultaneous amplification or damping of multiple modes [23, 24]. In the cases like energy transfer/harvesting and phonon lasing, where only one selected mode is interested, it is then quite straight forward to ask if amplifying only one mode while cooling all the other modes can be achieved via a single feedback loop.

In this Letter, we propose to use a single nonlinear feedback loop to realize the amplification of the lowest normal mode and the damping of all the other modes simultaneously in multimode mechanical systems. In the feedback-induced steady state, the phonon statistics indicate strong amplitude coherence in the lowest mode. The

phase coherence of the lowest mode is largely improved as well.

The amplification of the lowest modes and damping of all the other modes is closely related to the well-known Fröhlich condensate [25–34], where the vibration energy of a collection of oscillators would condensate in the lowest mode once the external energy supply exceeds a threshold. In Fröhlich condensate, the essential process is the energy redistribution among vibration modes induced by nonlinear couplings, whereas in our case it is through the nonlinear feedback.

*Model.* – We consider a mechanical resonator with several modes of oscillations. The configuration is shown in Fig. (1). The reflected and reference optical field from probe laser are collected by an interferometer to measure the collective displacement of the mechanical resonator. The measured displacement is then fed through a feedback loop to determine the drive applied onto the resonator. The feedback force can be provided by another laser via the optomechanical or photothermal effect, or by an electrical signal via the electromechanical effect.

The equations of motion (EOM) of the resonator are

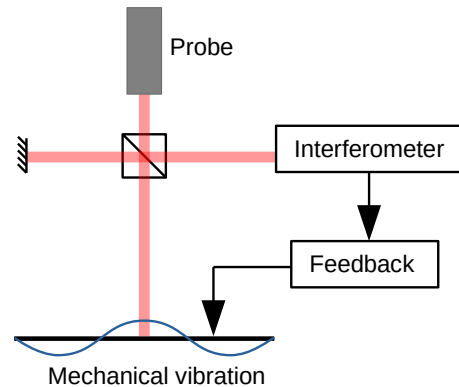


FIG. 1. Sketch of the multimode system considered. The reflected optical field provides information on the collective displacement of the resonator. Based on the detected signal, the feedback loop determines the drive applied onto the resonator. The feedback force can be realized using optomechanical, photothermal or electromechanical effect.

\* Xu.Zheng@Colorado.Edu

† Baowen.Li@Colorado.Edu

given by

$$\begin{aligned}\dot{Q}_j &= \omega_j P_j, \\ \dot{P}_j &= -\omega_j Q_j - \gamma_j P_j + \xi_j + H_{\text{fb}}^{(j)},\end{aligned}\quad (1)$$

where  $\omega_j$  is the frequency,  $Q_j = \sqrt{\frac{m}{k_B T}} \omega_j q_j$  and  $P_j = \frac{p_j}{\sqrt{m k_B T}}$  are the dimensionless displacement and momentum of the  $j$ th normal mode so that the dimensionless vibration energy  $\frac{1}{2}(Q_j^2 + P_j^2)$  at thermal equilibrium is equal to one,  $\gamma_j$  is the damping rate,  $\xi_j$  is the thermal noise and  $H_{\text{fb}}^{(j)}$  is the feedback force acted on the  $j$ th mode. At high temperature limit  $k_B T \gg \hbar \omega_j$ , the thermal noise satisfies  $\langle \xi_j(t) \xi_j(t') \rangle = 2\gamma_j \delta(t - t')$ . The feedback force  $H_{\text{fb}}^{(j)}$  is determined by the measured collective displacement  $Q = \sum_j Q_j$  of the resonator. To realize the condensation of phonons at the lowest mode, we design the feedback loop as follows:

$$\begin{aligned}F_I &= \int_0^t Q(s) ds, \\ F_D &= \dot{Q}, \\ H_{\text{fb}}^{(j)} &= -g_j \omega_{\text{fb}} \tanh[\omega_{\text{fb}}(F_I^2 F_D + 3Q^2 F_I)],\end{aligned}\quad (2)$$

where  $g_j$  is the feedback gain term and  $\omega_{\text{fb}}$  is a reference frequency to make  $H_{\text{fb}}^{(j)}$  have correct unit. The terms  $F_I$  and  $F_D$  are like the integral and derivative terms in the proportional–integral–derivative (PID) controller, which can be realized by the integrator and differentiator circuits, respectively. A hyperbolic tangent function is introduced to  $H_{\text{fb}}^{(j)}$  to limit the strength of the feedback force between  $\pm g_j \omega_{\text{fb}}$ . To understand how the feedback works, we first consider a simpler  $H_{\text{fb},0}^{(j)}$  where the hyperbolic tangent function is replaced by the identity function, i.e.,  $H_{\text{fb},0}^{(j)} = -g_j \omega_{\text{fb}}^2 (F_I^2 F_D + 3Q^2 F_I)$ . After introducing the complex amplitude

$$Q_j = \frac{1}{2} [a_j(t) e^{-i\omega_j t} + a_j^*(t) e^{i\omega_j t}] \quad (3)$$

with  $a_j(t)$  being slowly varying amplitudes ( $\dot{a}_j \ll \omega_j a_j$ ), we can simplify the amplitude equations as

$$\dot{a}_j = -\frac{\gamma_j}{2} a_j + \sum_i \frac{g_j \omega_{\text{fb}}^2}{4\omega_i^2 \omega_j} (\omega_i^2 - \omega_j^2) |a_i|^2 a_j + \Xi_j. \quad (4)$$

In the derivation we have assumed  $\omega_j \gg \gamma_j$ , ignored off-resonant terms and averaged the thermal noise  $\xi_j(t)$  over the fast dynamics,

$$\Xi_j(t) = \frac{\omega_j}{2\pi} \int_{t-\pi/\omega_j}^{t+\pi/\omega_j} ds \xi_j(s) e^{i\omega_j s}. \quad (5)$$

The slowly varying noise  $\Xi_j(t)$  satisfies

$$\langle \Xi_j(t) \Xi_j^*(t') \rangle = 2\gamma_j \delta(t - t'). \quad (6)$$

*Phonon condensation in the lowest mode.* – From the amplitude equations (4), we can define the effective damping rate

$$\tilde{\gamma}_j = \gamma_j + \sum_i \frac{g_j \omega_{\text{fb}}^2}{2\omega_i^2 \omega_j} (\omega_j^2 - \omega_i^2) |a_i|^2, \quad (7)$$

where the second term is induced by the nonlinear feedback and its sign depends on the frequencies of the modes. To gain an insight into the dynamics of the system, we first consider the case of  $N = 2$  modes. In this case, the second term is negative for the first mode [ $\text{sgn}(\omega_1^2 - \omega_2^2)$ ] and is positive for the second mode [ $\text{sgn}(\omega_2^2 - \omega_1^2)$ ], which means the damping rate of the first mode decreases ( $\tilde{\gamma}_1 < \gamma_1$ ) and that of the second mode increases ( $\tilde{\gamma}_2 > \gamma_2$ ). According to the approximate solution of the steady-state energy  $E_{j,ss} = \langle |a_j|^2 \rangle_{ss} / 2 \approx \gamma_j / \tilde{\gamma}_j$ , we can expect the steady-state energy of the first (second) mode to be greater (less) than that of the thermal equilibrium case, i.e.  $E_{1,ss} > 1 > E_{2,ss}$ . For the case of  $N > 2$  modes, it is straightforward to see  $\tilde{\gamma}_1 < \gamma_1$  since the feedback-induced term is always negative ( $\omega_1^2 - \omega_{i>1}^2 < 0$ ). Although a complete analysis of the other modes cannot be done, we can formulate a self-consistent statement by assuming the steady-state energy of the lowest mode is much larger than those of other modes, i.e. the phonon condensation can be achieved. In this limit, the dominant term introduced by the feedback force for the  $j$ th mode is the term proportional to  $(\omega_j^2 - \omega_1^2) |a_1|^2$ , which means the system with  $N > 2$  modes can be considered as a collection of systems with  $N = 2$  modes whose frequencies is  $\omega_1$  and  $\omega_j$ . Following the analysis of  $N = 2$  modes, we then obtain  $E_{1,ss} > 1 > E_{j,ss}$ , which is consistent with the assumption above.

While the analysis above is based on the feedback  $H_{\text{fb},0}^{(j)}$ , we find the feedback  $H_{\text{fb}}^{(j)}$  induces similar results, as shown by Fig. (2). The numerical results are obtained from the integration of Eq. (1) using SciML package [35]. Figure (2a) shows the time evolution of the vibration energy induced by the feedback  $H_{\text{fb}}^{(j)}$  in a system with  $N = 4$  modes. It is clearly seen that the vibration energy in the lowest mode is dominant at large times. The lowest mode is amplified by a factor of 10, while the other three modes are cooled to 0.57, 0.5 and 0.48, respectively. The ratio of vibration energy in the lowest mode to the total vibration energy is greater than 85% at steady state, as shown in Fig. (2b).

*Phonon statistics and coherence of the lowest mode.* – So far, we have only discussed the vibration energy in each mode and shown the feedback can give rise to the phonon condensation in the lowest mode. To gain more information about the feedback-induced steady state, we investigate the phonon statistics of the lowest mode. Figure (3a)-(3b) shows the phase portrait of the lowest mode without and with feedback. Without feedback, the phase portrait is peaked at the origin, which is consistent with the result of a thermal Brownian motion. With feedback, however, the phase portrait has a ring shape, which is

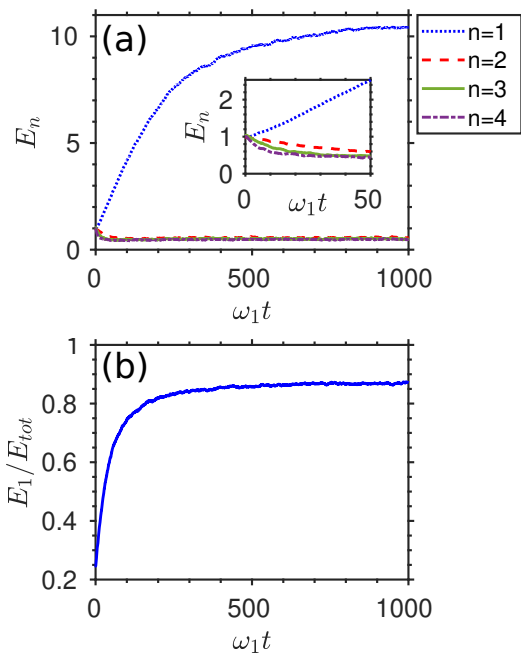


FIG. 2. (color online). Phonon condensation in a system with  $N = 4$  modes. (a) Vibration energy as a function of time. The dimensionless vibration energy at thermal equilibrium ( $t = 0$ ) is one. The inset is zoom-in. The lowest mode is amplified by a factor of 10, while the other three modes are cooled to 0.57, 0.5 and 0.48, respectively. (b) The ratio of vibration energy in the lowest mode to the total vibration energy of the system as a function of time. In our simulation, the frequencies of each mode are chosen according to the continuum elasticity theory  $\omega_j = kc_j$ , where  $c_j$ 's are obtained by solving the equation  $\cos \sqrt{c_j} \cosh \sqrt{c_j} = 1$  and  $k$  is a constant depending on the geometry and material of the resonator [36]. The first four modes satisfy  $\omega_2/\omega_1 = 2.75$ ,  $\omega_3/\omega_1 = 5.13$ ,  $\omega_4/\omega_1 = 8.75$ . The other parameters are  $\gamma_j/\omega_j = 10^{-2}$ ,  $g_j = g = 0.2$ ,  $\omega_{fb}/\omega_1 = 1$ .

similar to the phase portrait of a phonon laser [16, 37] and indicates the existence of amplitude coherence.

To give a further comparison of the phonon statistics without and with feedback, we show the phonon-number (energy) distribution of the lowest mode in Fig. (3c)-(3d). Without feedback, the phonon distribution follows the exponential distribution of thermal Boltzmann statistics. With feedback, the phonon distribution shifts from Boltzmann statistics to super-Poissonian statistics, where the most probable phonon number (energy) is non-zero. For an ideal coherent state, the variance of the phonon distribution is equal to the mean. The variance ( $\sim 19$ ) we obtained from Fig. (3d) is greater than the mean ( $\sim 10$ ), but it is much smaller than the variance ( $\sim 100$ ) of a thermal state with the same mean phonon number (energy), indicating the existence of strong thermal noise squeezing. The second order correlation function  $g^{(2)}(0)$  obtained from the phonon distribution is  $g^{(2)}(0) = \langle E_1^2 \rangle / \langle E_1 \rangle^2 = 1.17$ , which is close to the  $g^{(2)}(0)$  value of the coherent state.

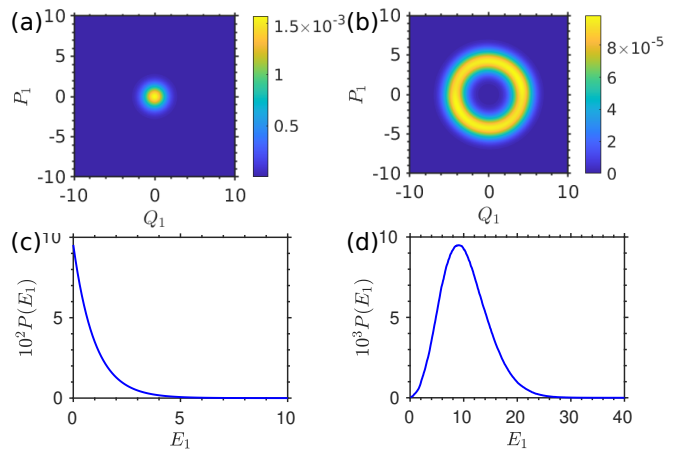


FIG. 3. (color online). Phonon statistics of the lowest mode at steady state. (a) Phase portrait of the lowest mode without feedback. (b) Phase portrait with feedback. (c) Phonon-number (energy) distribution without feedback. (d) Phonon-number (energy) distribution with feedback. The parameters used are the same as those in Fig. (2). The variance ( $\sim 19$ ) in (d) is much smaller than that ( $\sim 100$ ) in (c) of a thermal state with the same mean phonon number (energy).

By plotting the phase portrait, we show the amplitude coherence of the lowest mode in the feedback-induced steady state. We are also interested in the phase coherence, which can be determined by the linewidth of the noise power spectral density  $S_{Q_1 Q_1}(\omega)$ . The spectral density is obtained by the Fourier transform of autocorrelation function, i.e.,

$$S_{Q_1 Q_1}(\omega) = \int_{-\infty}^{+\infty} d\tau \overline{\langle Q_1(t) Q_1(t + \tau) \rangle} e^{i\omega\tau}, \quad (8)$$

where the overline denotes time average over  $t$  and the angle brackets denote ensemble average. Fig. (4) shows the spectral density  $S_{Q_1 Q_1}(\omega)$  without and with feedback. Without feedback, the intrinsic linewidth is  $\gamma_1/\omega_1 = 1 \times 10^{-2}$ , and the coherence time is given by  $\omega_1 \tau_{coh} = 2\omega_1/\gamma_1 = 200$ . With feedback, the linewidth is  $\tilde{\gamma}_1/\omega_1 = 7 \times 10^{-4}$ . The corresponding coherence time is  $\omega_1 \tilde{\tau}_{coh} = 2857$ , which is an order of magnitude longer than the intrinsic coherence time.

*Discussions and conclusions.* – The energy evolution in Fig. (2) is similar to the phonon number evolution in the formation of Fröhlich condensate [32, 34], illustrating the close connection between our model and Fröhlich condensate. This connection can be further seen from the similar formulas of the amplitude equations (4) and the rate equations of phonon numbers in Fröhlich's model (see Appendix A). In Fröhlich's model, there are third order terms in the Hamiltonian that couples the environment or auxiliary optical field with pairs of vibration modes [28–30, 34], inducing the energy redistribution among these modes. In our model, these interaction terms are replaced by the nonlinear feedback loop where a nonlinear functional of the collective motion  $Q = \sum_j Q_j$  induces

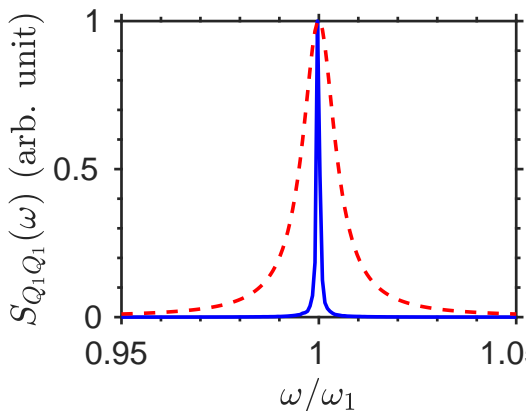


FIG. 4. (color online). Noise power spectral density of the lowest mode. For clear comparison, the spectral density has been rescaled so that the maximum value is 1. The blue solid line is the spectral density with feedback, and the red dashed line is the spectral density without feedback. With feedback, the linewidth is  $\tilde{\gamma}_1/\omega_1 = 7 \times 10^{-4}$ . Without feedback, the intrinsic linewidth is  $\gamma_1/\omega_1 = 1 \times 10^{-2}$ . The parameters used are the same as those in Fig. (2).

the interactions between different vibration modes. From this perspective, we provide a method to realize Fröhlich-like phonon condensation even in linear systems.

In summary, we have analyzed the prospects for using a feedback loop to realize the condensation of phonon or vibration energy in multimode mechanical systems. We have shown the proposed feedback decreases the effective damping rate of the lowest mode while increases the effective damping rate of other modes, which gives rise to the amplification of the lowest mode and the damping of all the other modes. For the phonon statistics and coherence of the lowest mode, the ring shape in the phase portrait, super-Poissonian phonon distribution and longer coherence time reveal intriguing similarities between the feedback-induced state and phonon laser. These features suggest the nonlinear feedback loop could be used in sensitive sensing and the design of novel monochromatic phonon laser where no two-level gain mediums are needed.

While we have used the continuum elasticity theory to model the mechanical resonator, the proposed feedback loop is applicable to general mechanical systems with incommensurable modes. The potential systems include nanoelectromechanical systems (NEMS), levitated nanoparticles in the optical tweezers, collective motions of cold atoms or ions in potential traps, etc. Further development from current model could replace the harmonic oscillators with more realistic nonlinear oscillators or self-sustained oscillators (e.g., Van der Pol oscillator). There are many interesting phenomena in coupled self-sustained oscillators, such as synchronization [38] and mode competition [39–41]. Our proposed feedback would be used in the control of these phenomena.

In our system, the essential part is the detailed form of

the feedback loop, which determines the capability and efficiency of achieving phonon or energy condensation. While the proposed one works well, other feedback strategies might provide similar or even better results. Looking for better feedback strategies, especially with the help of the fast-developing machine learning models, is a promising direction [42]. Besides, the effect of a time delay and phase difference in the feedback loop is an interesting topic and deserves further study.

### Appendix A: Comparison of our model and Fröhlich's model

The rate equations of phonon numbers in Fröhlich's model are given by

$$\begin{aligned} \dot{n}_j = & s - \gamma_j(n_j - \bar{n}_{j,\text{th}}) \\ & + \chi \sum_i [(n_j + 1)n_i - n_j(1 + n_i)e^{\hbar(\omega_j - \omega_i)/k_B T}], \end{aligned} \quad (\text{A1})$$

where  $s$  is the external pumping,  $\chi$  is the coupling strength of two-phonon process,  $\bar{n}_{j,\text{th}}$  is the thermal phonon number. In the limit of large phonon number  $n_j \gg 1$ , the equations are simplified as

$$\dot{n}_j = s - \gamma_j(n_j - \bar{n}_{j,\text{th}}) + \chi \sum_i [1 - e^{\hbar(\omega_j - \omega_i)/k_B T}] n_i n_j. \quad (\text{A2})$$

Recently, there is a proposal to realize Fröhlich condensate in optomechanical systems [34]. The modified rate equations of phonon numbers are given by

$$\begin{aligned} \dot{n}_j = & -\gamma_j(n_j - \bar{n}_{j,\text{th}}) \\ & + \sum_{i \neq j} 4U_{i,j}^2 [\Gamma(\omega_i - \omega_j) - \Gamma(\omega_j - \omega_i)] n_i n_j, \end{aligned} \quad (\text{A3})$$

where  $U_{i,j}$  is coefficient and  $\Gamma(\omega)$  is a function of frequency. To compare the amplitude equations (4) with Eq. (A2) and (A3), we need to convert Eq. (4) to the rate equations of  $\langle |a_j(t)|^2 \rangle$ . The formal solution of Eq. (4) is given by

$$\begin{aligned} a_j(t) = & \int_{-\infty}^t ds e^{-\frac{\gamma_j}{2}(t-s) + \sum_i \frac{g_j \omega_{\text{fb}}^2}{4\omega_i^2 \omega_j} (\omega_i^2 - \omega_j^2) \int_s^t dt' |a_i(t')|^2} \Xi_j(s) \end{aligned} \quad (\text{A4})$$

From Eq. (A4) we can get the formal solution of  $\langle |a_j(t)|^2 \rangle$ ,

$$\begin{aligned} \langle |a_j(t)|^2 \rangle & \approx 2\gamma_j \int_{-\infty}^t ds \langle e^{-\gamma_j(t-s) + \sum_i \frac{g_j \omega_{\text{fb}}^2}{4\omega_i^2 \omega_j} (\omega_i^2 - \omega_j^2) \int_s^t dt' |a_i(t')|^2} \rangle, \end{aligned} \quad (\text{A5})$$

where we have used Eq. (6) and decorrelation approximation. Hence, the rate equations of  $\langle |a_j(t)|^2 \rangle$  are given by

$$\begin{aligned} \frac{d\langle |a_j|^2 \rangle}{dt} \approx & -\gamma_j(\langle |a_j|^2 \rangle - 2) \\ & + \sum_i \frac{g_j \omega_{\text{fb}}^2}{4\omega_i^2 \omega_j} (\omega_i^2 - \omega_j^2) \langle |a_i|^2 \rangle \langle |a_j|^2 \rangle \end{aligned} \quad (\text{A6})$$

under decorrelation approximation. In the high temperature limit, the phonon numbers are determined by  $n_j = \langle |a_j|^2 \rangle k_B T / (2\hbar\omega_j)$ . From Eq. (A6), the rate equations of phonon numbers in our model are then given by

$$\dot{n}_j \approx -\gamma_j(n_j - \bar{n}_{j,\text{th}}) + \sum_i \frac{\hbar g_j \omega_{\text{fb}}^2}{2k_B T \omega_i \omega_j} (\omega_i^2 - \omega_j^2) n_i n_j \quad (\text{A7})$$

Eq. (A7) has the same form as Eq. (A2) and (A3) except the coupling function before  $n_i n_j$  is different and there is no external pumping when compared with Eq. (A2).

- 
- [1] T. Dekorsy, G. C. Cho, and H. Kurz, Coherent phonons in condensed media, *Light scattering in solids VIII* **76**, 169 (2000).
- [2] P. Ruello and V. E. Gusev, Physical mechanisms of coherent acoustic phonons generation by ultrafast laser action, *Ultrasonics* **56**, 21 (2015).
- [3] C. L. Poyser, A. V. Akimov, R. P. Champion, and A. J. Kent, Coherent phonon optics in a chip with an electrically controlled active device, *Sci. Rep.* **5**, 1 (2015).
- [4] R. Ruskov and C. Tahan, Coherent phonons as a new element of quantum computing and devices, in *J. Phys. Conf. Ser.*, Vol. 398 (IOP Publishing, 2012) p. 012011.
- [5] M. V. Gustafsson, T. Aref, A. F. Kockum, M. K. Ekström, G. Johansson, and P. Delsing, Propagating phonons coupled to an artificial atom, *Science* **346**, 207 (2014).
- [6] A. Bienfait, K. J. Satzinger, Y. Zhong, H.-S. Chang, M.-H. Chou, C. R. Conner, É. Dumur, J. Grebel, G. A. Peairs, R. G. Povey, *et al.*, Phonon-mediated quantum state transfer and remote qubit entanglement, *Science* **364**, 368 (2019).
- [7] J. Liu, H. Guo, and T. Wang, A review of acoustic metamaterials and phononic crystals, *Crystals* **10**, 305 (2020).
- [8] T. Takabatake, K. Suekuni, T. Nakayama, and E. Kaneshita, Phonon-glass electron-crystal thermoelectric clathrates: Experiments and theory, *Rev. Mod. Phys.* **86**, 669 (2014).
- [9] N. Li, J. Ren, L. Wang, G. Zhang, P. Hänggi, and B. Li, Colloquium: Phononics: Manipulating heat flow with electronic analogs and beyond, *Rev. Mod. Phys.* **84**, 1045 (2012).
- [10] Y. Li, W. Li, T. Han, X. Zheng, J. Li, B. Li, S. Fan, and C.-W. Qiu, Transforming heat transfer with thermal metamaterials and devices, *Nat. Rev. Mater.* **6**, 488 (2021).
- [11] D. Rugar, R. Budakian, H. Mamin, and B. Chui, Single spin detection by magnetic resonance force microscopy, *Nature* **430**, 329 (2004).
- [12] Y.-T. Yang, C. Callegari, X. Feng, K. L. Ekinci, and M. L. Roukes, Zeptogram-scale nanomechanical mass sensing, *Nano Lett.* **6**, 583 (2006).
- [13] T. P. Burg, M. Godin, S. M. Knudsen, W. Shen, G. Carlson, J. S. Foster, K. Babcock, and S. R. Manalis, Weighing of biomolecules, single cells and single nanoparticles in fluid, *Nature* **446**, 1066 (2007).
- [14] S. C. Masmanidis, R. B. Karabalin, I. De Vlaminck, G. Borghs, M. R. Freeman, and M. L. Roukes, Multifunctional nanomechanical systems via tunably coupled piezoelectric actuation, *Science* **317**, 780 (2007).
- [15] X. Feng, C. White, A. Hajimiri, and M. L. Roukes, A self-sustaining ultrahigh-frequency nanoelectromechanical oscillator, *Nat. Nanotechnology* **3**, 342 (2008).
- [16] Y. Wen, N. Ares, F. Schupp, T. Pei, G. Briggs, and E. Laird, A coherent nanomechanical oscillator driven by single-electron tunnelling, *Nat. Physics* **16**, 75 (2020).
- [17] I. Mahboob and H. Yamaguchi, Bit storage and bit flip operations in an electromechanical oscillator, *Nat. Nanotechnology* **3**, 275 (2008).
- [18] Q. P. Unterreithmeier, E. M. Weig, and J. P. Kotthaus, Universal transduction scheme for nanomechanical systems based on dielectric forces, *Nature* **458**, 1001 (2009).
- [19] Y. Tadokoro, H. Tanaka, and M. Dykman, Driven nonlinear nanomechanical resonators as digital signal detectors, *Sci. Rep.* **8**, 1 (2018).
- [20] J. Tamayo, A. Humphris, R. Owen, and M. Miles, High-Q dynamic force microscopy in liquid and its application to living cells, *Biophys. J.* **81**, 526 (2001).
- [21] G. S. Shekhawat and V. P. Dravid, Nanoscale imaging of buried structures via scanning near-field ultrasound holography, *Science* **310**, 89 (2005).
- [22] L. Tetard, A. Passian, K. T. Venmar, R. M. Lynch, B. H. Voy, G. Shekhawat, V. P. Dravid, and T. Thundat, Imaging nanoparticles in cells by nanomechanical holography, *Nat. Nanotechnology* **3**, 501 (2008).
- [23] R. Ohta, H. Okamoto, and H. Yamaguchi, Feedback control of multiple mechanical modes in coupled micromechanical resonators, *Appl. Phys. Lett.* **110**, 053106 (2017).
- [24] C. Sommer and C. Genes, Partial optomechanical refrigeration via multimode cold-damping feedback, *Phys. Rev. Lett.* **123**, 203605 (2019).
- [25] H. Fröhlich, Bose condensation of strongly excited longitudinal electric modes, *Phys. Lett. A* **26**, 402 (1968).
- [26] H. Fröhlich, Long-range coherence and energy storage in biological systems, *Int. J. Quantum Chem.* **2**, 641 (1968).
- [27] H. Fröhlich, Long range coherence and the action of enzymes, *Nature* **228**, 1093 (1970).
- [28] T. Wu and S. Austin, Bose condensation in biosystems, *Phys. Lett. A* **64**, 151 (1977).
- [29] T. Wu and S. Austin, Cooperative behavior in biological systems, *Phys. Lett. A* **65**, 74 (1978).

- [30] T. Wu and S. J. Austin, Fröhlich's model of Bose condensation in biological systems, *J. Biol. Phys.* **9**, 97 (1981).
- [31] J. R. Reimers, L. K. McKemmish, R. H. McKenzie, A. E. Mark, and N. S. Hush, Weak, strong, and coherent regimes of Fröhlich condensation and their applications to terahertz medicine and quantum consciousness, *Proc. Nat. Acad. Sci.* **106**, 4219 (2009).
- [32] J. Preto, Semi-classical statistical description of Fröhlich condensation, *J. Biol. Phys.* **43**, 167 (2017).
- [33] Z. Zhang, G. S. Agarwal, and M. O. Scully, Quantum fluctuations in the Fröhlich condensate of molecular vibrations driven far from equilibrium, *Phys. Rev. Lett.* **122**, 158101 (2019).
- [34] X. Zheng and B. Li, Fröhlich condensate of phonons in optomechanical systems, *Phys. Rev. A* **104**, 043512 (2021).
- [35] C. Rackauckas and Q. Nie, Differentialequations.jl—a performant and feature-rich ecosystem for solving differential equations in julia, *J. Open Res. Softw.* **5** (2017).
- [36] L. D. Landau, L. P. Pitaevskii, A. M. Kosevich, and E. M. Lifshitzch, *Course of Theoretical Physics: Theory of Elasticity* (Pergamon press, 1986).
- [37] R. M. Pettit, W. Ge, P. Kumar, D. R. Luntz-Martin, J. T. Schultz, L. P. Neukirch, M. Bhattacharya, and A. N. Vamivakas, An optical tweezer phonon laser, *Nat. Photonics* **13**, 402 (2019).
- [38] A. Pikovsky, M. Rosenblum, and J. Kurths, *Synchronization: a universal concept in nonlinear sciences*, Vol. 12 (Cambridge University Press, 2003).
- [39] L. M. Jonsson, F. Santandrea, L. Y. Gorelik, R. I. Shekhter, and M. Jonson, Self-organization of irregular nanoelectromechanical vibrations in multimode shuttle structures, *Phys. Rev. Lett.* **100**, 186802 (2008).
- [40] U. Kemiktarak, M. Durand, M. Metcalfe, and J. Lawall, Mode competition and anomalous cooling in a multimode phonon laser, *Phys. Rev. Lett.* **113**, 030802 (2014).
- [41] X. Zhang, T. Lin, F. Tian, H. Du, Y. Zou, F. S. Chau, and G. Zhou, Mode competition and hopping in optomechanical nano-oscillators, *Appl. Phys. Lett.* **112**, 153502 (2018).
- [42] C. Sommer, M. Asjad, and C. Genes, Prospects of reinforcement learning for the simultaneous damping of many mechanical modes, *Sci. Rep.* **10**, 1 (2020).